Separation of stochastic and deterministic California subsurface currents from Lagrangian drifter using the Hilbert-Huang transform

Peter C. Chu, Naval Postgraduate School, Monterey, CA 93943

INTRODUCTION

The empirical mode decomposition (EMD) (Huang et al., 1998) was used to separate a Lagrangian trajectory into low-frequency (non-diffusive, i.e., deterministic) and high-frequency (diffusive, i.e., stochastic) components. The 2D turbulent (or called eddy) diffusion coefficients are calculated on the base of the classical turbulent diffusion with mixing length theory from stochastic component of a single drifter.

EMPIRICAL MODE DECOMPOSITION

Mathematically, there are infinite number of ways to decompose a functions into a complete set of components.

The ones that give us more physical insight are more significant.
In general, the few the number of representing components, the higher the information content.

The adaptive method will represent the characteristics of the signal better.

EMD is an adaptive method that can generate infinite many sets of IMF components to represent the original data.

Figure 1. Empirical mode decomposition.

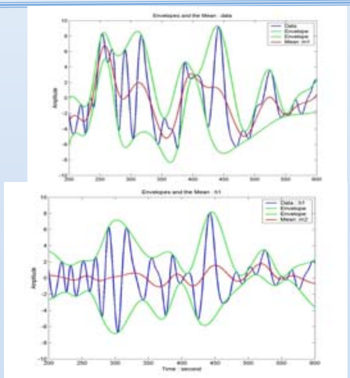

$$x(t) - m_1 = h_1 ,$$

$$h_1 - m_2 = h_2 = x(t) - (m_1 + m_2)$$

.....

.....

$$h_{k-1} - m_k = h_k = x(t) - (m_1 + m_2 + \ldots + m_k)$$

$$\Rightarrow \quad h_k = c_1 .$$

STOCHASEIC LAGRANGIAN VELOCITY

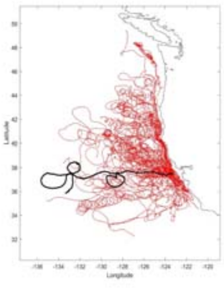

Figure 2. Trajectories of 54 RAFOS floats in the California coast by the Naval Postgraduate School between 1992 and 2004. The thick black trajectory refers to the Float N035.

(http://www.oc.nps.edu/npsRAFOS/).

$$\mathbf{x}(t_j) = \mathbf{x}_{\det}(t_j) + \mathbf{x}_{sto}(t_j), \quad j = 1, 2, \ldots, J$$

$$u_{sto}(t_j) = \frac{x_{sto}(t_{j+1}) - x_{sto}(t_{j-1})}{t_{j+1} - t_{j-1}}, \quad j = 2, 3, \ldots, J\text{-}1$$

$$\delta_x = \sqrt{\frac{1}{J}\sum_{j=1}^{J} x_{sto}^2(t_j)}, \quad \delta_y = \sqrt{\frac{1}{J}\sum_{j=1}^{J} y_{sto}^2(t_j)} \quad \sigma_x = \sqrt{\frac{1}{J}\sum_{j=1}^{J} u_{sto}^2(t_j)}, \quad \sigma_y = \sqrt{\frac{1}{J}\sum_{j=1}^{J} v_{sto}^2(t_j)}$$

$$K_x = c\sigma_u\delta_x, \quad K_y = c\sigma_v\delta_y, \quad c = 0.1 \text{ (Ozmidov Coefficient)}$$

EMD OF THE RAFOS FLOAT N035

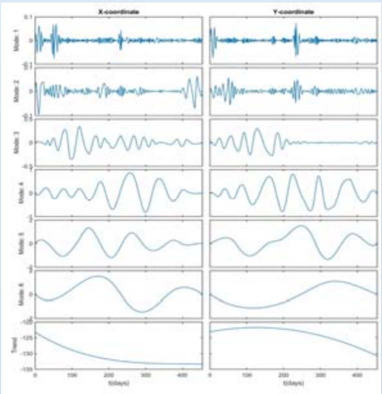

Figure 3. IMFs and trend for (a) x(t), and (b) y(t) of the RAFOS N035.

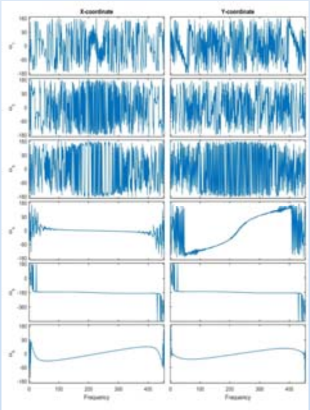

Figure 4. The phase spectra for the IMFs in Figure 3.

IDENTIFICATION OF STOCHASTIC VELOCITY

$$f_{pk} = \frac{1}{J}\sum_{t=0}^{J-1} c_p(t)\exp\left[(-i2\pi k/J)t\right], \quad k = 0, 2, \ldots, J-1 \quad \theta_p(k) = \arctan\frac{\mathrm{Im}(f_{pk})}{\mathrm{Re}(f_{pk})}$$

$$a_p(k) = \sqrt{\left|f_{pk}\hat{f}_{pk}\right|}/J, \quad k = 1, 2, \ldots, J/2 \qquad E_{p,\alpha} = \sum_{k=1}^{m} a_p^2(k), \quad E_{p,T} = \sum_{k=1}^{J/2} a_p^2(k)$$

$$\Gamma_{p,\alpha} = R_{p+1,\alpha} / R_{p,\alpha} \qquad \Gamma_{s,\alpha} = \max(\Gamma_{p,\alpha} \mid p = 1, 2, \ldots, P-1)$$

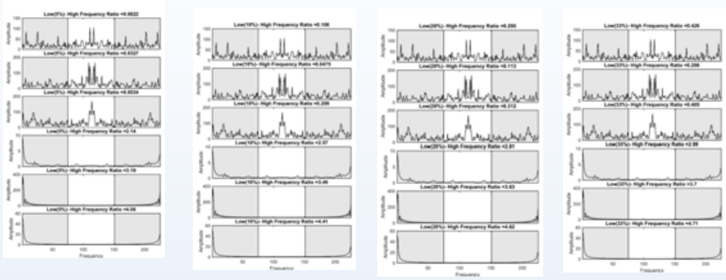

(a) 5% (b 10%, (c) 20% (d) 33%

Figure 5. Combination of IFM-4, IMF-5, IFM-6, and trend constitutes the deterministic component

TURBULENT DIFFUSION COEFFICIENTS FOR EACH FLOAT

Table 1. Horizontal diffusivity coefficients (K_x, K_y) identified from each RAFOS float

Float	K_x (m²/s)	K_y (m²/s)	Float	K_x (m²/s)	K_x (m²/s)
N002	50.33	35.36	N050	807.00	869.98
N003	201.50	256.01	N051	1,428.79	429.88
N004	1,268.10	961.34	N053	744.84	567.72
N005	512.28	161.15	N055	575.79	1,266.25
N006	1,154.57	491.32	N062	527.90	455.62
N007	140.41	322.12	N063	264.97	159.00
N008	229.77	136.26	N064	857.32	317.78
N010	275.39	239.34	N065	236.35	78.13
N011	249.02	243.60	N066	928.46	816.23
N013	402.84	331.44	N067	1,113.50	1,064.76
N014	357.15	310.99	N069	542.80	255.66
N019	530.12	692.70	N071	90.03	217.50
N021	66.89	13.61	N072	540.54	464.90
N022	15.08	10.28	N073	506.08	431.43
N024	46.75	10.07	N075	1,190.04	1,128.97
N026	788.09	180.61	N080	1,119.79	1,052.69
N028	301.14	146.19	N081	919.83	1,118.54
N029	128.14	227.37	N082	690.91	893.65
N030	20.37	438.64	N083	1,216.25	1,535.29
N031	1,372.19	1,354.11	N084	768.98	683.10
N032	375.76	284.72	N085	971.53	1,357.00
N033	106.38	662.16	N087	604.49	904.98
N035	896.11	330.70	N088	488.44	1,323.34
N039	539.05	631.89	N089	762.60	2,579.02
N041	1,123.98	619.72	N090	1,803.36	2,067.87
N043	1,057.78	618.90	N091	931.87	838.59
N048	476.43	86.36	N092	969.12	1,277.95

SUMMARY

This study shows the capability of EMD to decompose a single drifter's trajectory into deterministic and stochastic components. This will largely improve the Lagrangian observations. This method can be used in general signal processing.

REFERENCES

Chu, P.C., 2018: Steepest ascent low/non-low frequency ratio in empirical mode decomposition to separate deterministic and stochastic velocities from a single Lagrangian drifter. Journal of Geophysical Research, in press.

Chu, P.C., C.W. Fan, and N. Huang, 2014: Derivative-optimized empirical mode decomposition for the Hilbert-Huang transform. *Journal of Computational and Applied Mathematics*, **259**, 57-64.

Chu, P.C., C.W. Fan, and N. Huang, 2012: Compact empirical mode decomposition— an algorithm to reduce mode mixing, end effect, and detrend uncertainty. *Advances in Adaptive Data Analysis*, **4** (3) 1250017 (18 pages) doi: 10.1142/S1793536912500173.

Correspondence: Peter C. Chu, Department of Oceanography, Naval Postgraduate School, Monterey, California, USA (pcchu@nps.edu)

Acknowledgements. **This study has been sponsored by ONR, NAVO, and the U.S. Navy.**